Science of the Total Environment 621 (2018) 177–185

Contents lists available at ScienceDirect

Science of the Total Environment

journal homepage: www.elsevier.com/locate/scitotenv

Identifying change in spatial accumulation of soil salinity in an inland river watershed, China

Yugang Wang [a,*], Caiyun Deng [a,b], Yan Liu [a], Ziru Niu [a,b], Yan Li [a]

[a] State Key Laboratory of Desert and Oasis Ecology, Xinjiang Institute of Ecology and Geography, Chinese Academy of Sciences, Urumqi, Xinjiang 830011, China
[b] University of Chinese Academy of Sciences, Beijing 100049, China

HIGHLIGHTS

- We investigated the spatial change of salt accumulation in soil.
- 56% of the studied area experienced changes in soil salt content.
- The Lorenz curve was applied to soil salinity accumulation across a watershed.
- Soil salt accumulation per unit area increased by about 16%.
- Results provide an insight into the spatial patterns of soil salinity accumulation.

GRAPHICAL ABSTRACT

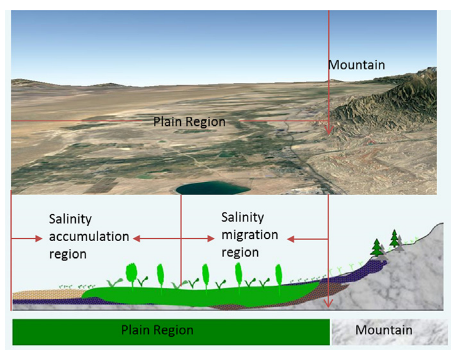

ARTICLE INFO

Article history:
Received 16 August 2017
Received in revised form 18 October 2017
Accepted 20 November 2017
Available online xxxx

Editor: G. Ashantha Goonetilleke

Keywords:
Soil salinization
Land use
Arid land
Soil salinity variation
Lorenz curve
Geostatistics

ABSTRACT

Soil salinity accumulation is strong in arid areas and it has become a serious environmental problem. Knowledge of the process and spatial changes of accumulated salinity in soil can provide an insight into the spatial patterns of soil salinity accumulation. This is especially useful for estimating the spatial transport of soil salinity at the watershed scale. This study aimed to identify spatial patterns of salt accumulation in the top 20 cm soils in a typical inland watershed, the Sangong River watershed in arid northwest China, using geostatistics, spatial analysis technology and the Lorenz curve. The results showed that: (1) soil salt content had great spatial variability (coefficient variation > 1.0) in both in 1982 and 2015, and about 56% of the studied area experienced transition the degree of soil salt content from one class to another during 1982–2015. (2) Lorenz curves describing the proportions of soil salinity accumulation (SSA) identified that the boundary between soil salinity migration and accumulation regions was 24.3 m lower in 2015 than in 1982, suggesting a spatio-temporal inequality in loading of the soil salinity transport region, indicating significant migration of soil salinity from the upstream to the downstream watershed. (3) Regardless of migration or accumulation region, the mean value of SSA per unit area was 0.17 kg/m^2 higher in 2015 than 1982 ($p < 0.01$) and the increasing SSA per unit area in irrigated land significantly increased by 0.19 kg/m^2 compared with the migration region. Dramatic accumulation of soil salinity in all land use types was clearly increased by 0.29 kg/m^2 in this agricultural watershed during the studied period in the arid northwest of China. This study demonstrates the spatial patterns of soil salinity accumulation, which is particularly useful for estimating the spatial transport of soil salinity at the watershed scale.

* Corresponding author.
E-mail address: wangyg@ms.xjb.ac.cn (Y. Wang).

https://doi.org/10.1016/j.scitotenv.2017.11.222
0048-9697/

1. Introduction

Soil salinization is a global issue, especially in arid and semiarid areas with low rainfall and high evapotranspiration (Butcher et al., 2016; Amundson et al., 2015; Li et al., 2014). Soil salinization influences soil quality and the sustainability of agriculture, and can decrease biodiversity, and reduce water quality and agricultural production (Cassel et al., 2015; Aragüés et al., 2014; Bui, 2013). An area of >930 million ha that occupies 7% of global land surface suffers from soil salinization, and the area is expanding (Rengasamy, 2006). Approximately 20% of irrigated land is salt-affected globally (Yeo, 1999), and the land area that has secondary soil salinization problems is as high as about 80 million ha in arid and semiarid regions (Ghassemi et al., 1997). Hence, it is crucial to mitigate and control soil salinity in agricultural lands, particularly where irrigation is used (Jalila et al., 2016; Singh, 2015). Understanding the process and spatial changes of salt accumulation in soil will improve ways to prevent soil degradation, and ameliorate soil quality for economic development (Salvati and Ferrara, 2015). This asks for accurate estimation of spatial variation of soil salinization at large scales (Daliakopoulos et al., 2016; Sheng et al., 2010; Benyamini et al., 2005).

Understanding the accumulation patterns and processes of soil salinity and its correlative factors is crucial to control soil salinization in arid environments. Previous studies showed that human activities and climate change are the primary controls on soil secondary salinization (Zhou et al., 2013; Foley et al., 2011). The conversion of natural land use (e.g. grasslands and forests) to cropland has dramatically affected soil properties as well as their spatial and temporal patterns. These changes often accelerate soil salinization (Abliz et al., 2016; Devkota et al., 2015; Ibrakhimov et al., 2011; Beltran, 1999). Generally, the spatial variation of soil salinity is substantially regulated by factors such as topography, climate and hydrological conditions (Yang et al., 2016; Wang and Li, 2013; Wang et al., 2008a). Soil salts are transported and redistributed with soil water, groundwater and irrigation water across the landscape. This process is significant in surface soils under conditions of little precipitation and high evapotranspiration in arid environments (Pankova et al., 2015; Zhang et al., 2014a; Cetin and Kirda, 2003). Therefore, better understanding about the spatial patterns of soil salinity could inform scientific strategies to control salinization for sustainable land management (Taghizadeh-Mehrjardi et al., 2014; Bennett et al., 2010; Qadir and Oster, 2004).

Current studies often estimate soil salinity change using indirect measurements, small-scale experiments or poorly defined periods of time (Herrero and Pérez-Coveta, 2005). Although single field investigations or observations can give some information about short-term changes in soil salinity (Scudiero et al., 2017), the changes in soil salinity are related not only among fields, but also irrigation regions and even the entire watershed (Scudiero et al., 2016; Zhang et al., 2014b). Clearly such limited information is inadequate to explain comprehensive soil–landscape relationships concerning transport and accumulation of soil salinity among irrigation regions, especially at the watershed scale. Quantifying the spatio-temporal variation of soil properties at larger scales is critical to adequately understand the extent of the environment problem (Corwin et al., 2006). However, it is a major challenge to quantify the spatio-temporal patterns of soil salinity accumulation (SSA) in heterogeneous soils.at the watershed scale.

Techniques and methods to monitor and map soil salinization have been a focus for research in arid and semiarid areas in recent years, because they are crucial for effective land management and utilization (Lal, 2015; Nurmemet et al., 2015; Cruz-Cárdenas, 2014; Ding et al., 2011; Fernandez-Buces et al., 2006). The appropriate mapping methods depend on the spatial scale of interest. Geostatistics, as an effective tool to study and predict the spatial structure of geo-referenced variables, has been commonly used to map soil salinization (Niñerola et al., 2017; Li H.Y. et al., 2015; Li Y. et al., 2015; Juan et al., 2011; Douaik et al., 2005; Pozdnyakova and Zhang, 1999). It was used to describe spatial variability for a number of natural indexes (Monestiez et al., 2010; Renard et al., 2005; Cambardella et al., 1994), as well as the temporal and spatial characteristics of soil properties over a large area (Tripathi et al., 2015). Therefore, identifying the spatial change of soil salt migration and accumulation is helpful to control soil salinization at the watershed scale. The Lorenz curve, defined by M.E. Lorenz (1905), is commonly used to describe the degree of inequality in social distribution of income and has become an effective statistical measurement for general equality analysis (Chakravarty, 1990). In recent years, this has gradually been introduced to resource and environment fields, and has proved effective in illuminating imbalances in distributions (Abell et al., 2013; Chen et al., 2009; Preston et al., 1989). The distribution of salt accumulation in soil is highly heterogeneous in the process of loading of soil salinity transport in the space of watershed. The Lorenz curve can be applied to soil salinity data to determine tradeoffs in the regions of soil salinity migration and accumulation, using the Gini coefficient as the criterion. Thus, the combination of information from the Lorenz curve and geostatistical analyses of soil salinity allows assessment of soil salinity accumulation in transport and accumulation regions, which advance our understanding of the spatio-temporal pattern of soil salinization during the long-term process of land use at the watershed scale.

The Sangong River watershed, a well-known inland river watershed in China's Xinjiang Province, was selected as a case study. This study aims (1) to quantify spatial variability of soil salinity at the watershed scale during 1982–2015, (2) to identify the boundary of soil salinity migration and accumulation regions using the Lorenz curve and (3) to assess the degree of soil salinity accumulation in different regions across land use types.

2. Materials and methods

2.1. Site description

The Sangong River watershed (87°49′–88°16′E, 43°50′–44°22′N) is located in the northern Tianshan Mountains and southern the Guerbantonggute Desert in northwest China (Fig. 1). The watershed covers mountainous region in the south and plains in the north. The plain region in this watershed is for agricultural use. It covers an area of 94,200 ha, and the north–south and east–west distances are 36.97 and 37.65 km, respectively; with the slope of only 2–2.5% downwards from south to north. The elevation varies from 710 m in the south to 440 m in the north (Fig. 1). The climate in the region is the arid continental climate, and the mean annual precipitation is <200 mm and mean annual temperature 7.3 °C with average maximum of 25.75 °C in July and average minimum of 15.7 °C in January. Based on long-term meteorological data (1965–2005), the mean annual pan evaporation is about 1533–2240 mm. In this area, irrigation is essential for agriculture due to little precipitation and high evapotranspiration. The dominant land use type is irrigated agriculture, with urban areas accounting for only a small percentage of the study area. The main soil classes are Solonchak, Haplic calcisols and Aquert, and they have been affected by agricultural practices for over 50 years. The crops in the region include wheat, corn, cotton, grapes and hops. This region has experienced intensive land exploitation since the 1960s and soil salinization has become a serious environmental problem during to irrigation (Wang et al., 2008b). Natural vegetation in the study region includes a variety of xeromorphic formations, e.g. *Reaumuria soongorica*, *Salsola nitraria*, *Ceratocarpus arenarius*, *Tamarix ramosissima*, etc.

2.2. Data source and processing

Soil salt content in 1982 and 2015 was obtained in two ways: we collected and measured soil salt content of 290 soil samples in 2015, and the other 145 data points in 1982 were from China's National Soil Inventory in the Sangong River watershed (Fukang Land Resources Administration, 1983). The locations of soil samples in 1982 were

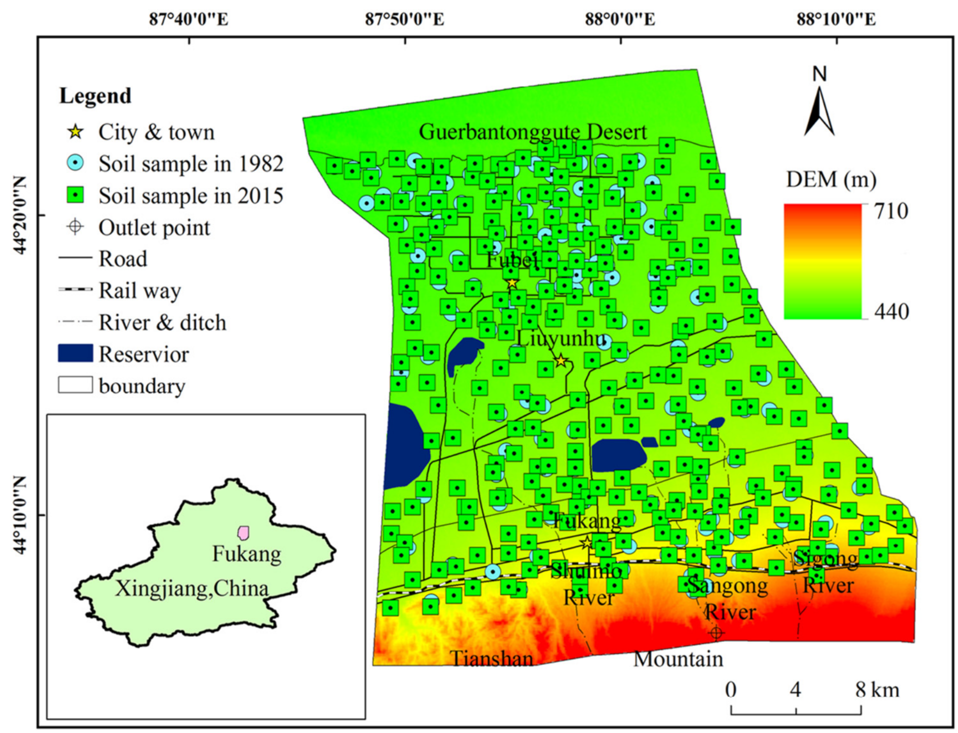

Fig. 1. Location, topography, and the sampling sites of the Sangong River watershed.

recorded by geographic situation and land cover information. In 2015, the surface soils (0–20 cm) were collected according to the national soil inventory method, and sampling locations were recorded using GPS. We gridded the sampling area by 2.5 km × 2.5 km; and then collected at least one sample in each grid of the main plain region. The elevation of sampling points varies from 636 m in the south to 456 m in the north. Soils were collected in different directions using a hand soil auger from 3–5 randomly selected spots within each land parcel, and then compiled as one sample. Soil samples were air dried, crushed passed through a 2-mm mesh and the large debris, plant roots, stones and other gravel-sized materials were removed by hand. The salt content of all soil samples was analyzed using the suspensions of 1:5 soil: water ratio. We measured Na^+, K^+, Ca^{2+}, Mg^{2+}, SO_4^{2+}, Cl^-, CO_3^{2-}, and HCO_3^- and then calculated the soil salt content as the sum of the eight element (Bao, 2000).

Land use types were obtained using a land-use map at a scale of 1:50,000 for 1982 and 2015 (Fukang Land Resource Administration, 2015). According to impacts of human activity on soil salinity, land use in the study area was divided into irrigated and non-irrigated land, which includes eight types: cropland, grassland, planted forest, reservoir/flood land, shrub land, saline land, sandy desert, and construction land (Fig. S1). Irrigated land includes cropland, planted forest, and non-irrigated land includes grassland, shrub land, saline land, and sandy desert. In this study, linear characteristic such as riverbeds, ditches, roads and railway was not individually classified in land use types (Fig. S1).

2.3. Statistical analysis

Descriptive statistical analyses for mean, standard deviation, minimum and maximum values, coefficient of variation (CV), kurtosis and skewness were applied to the results from soil samples in 1982 and 2015. The Kolmogorov–Smirnov (K–S) test was used to test whether soil salt content was normally distributed. We used the software package SPSS 20.0 for Windows for all the conventional statistical analyses (SPSS Inc., Armonk, NY, USA).

Geostatistical methods provide a series of statistical ways to combine the observed data and the soil properties' variation in space and time through a random process (Goovaerts, 1999). Thus, one significant contribution of geostatistics is a map of the probability of soil salinity values (Castrignano et al., 2002). The semivariogram represents the relationship each point between its neighbor as the spatial dependence. It generally follows the equation:

$$\gamma(h) = \frac{1}{2N(h)} \sum_{i=1}^{N(h)} [z(x_i) - z(x_i + h)]^2 \tag{1}$$

where $\gamma(h)$ refers a semivariogram value; h refers the step length, which is the spatial interval of sampling points for the classification to reduce the individual number of spatial distances of various sampling point assemblages; $z(x_i)$ and $z(x_i + h)$ refer the measured values at sampling points x_i and $x_i + h$; and $N(h)$ refers the number of pairs separated by lag h.

The ordinary kriging is a method as an un-sampled site, which usually shows a weighted observations within a neighborhood and an ideal method of spatial prediction:

$$Z(x_0) = \sum_{i=1}^{n} \lambda_i Z(x_i) \tag{2}$$

where $z(x_0)$ refers the estimated value at the location x_0, λ_i refers the weight assigned to the i^{th} observation, $z(x_i)$ refers the known value at the sampling point x, and n is the number of sites within the search neighborhood for the estimate and is based on the size of the moving window which is defined by users.

Validation of predicated map of soil salt content was tested using two indices (the mean error (ME) and the root mean square standardized error (RMSSE)) to assess the effectiveness of kriging. When the ME is close to 0 and the RMSSE close to 1, the predicted map of soil salt content is credible in the study area (Kitanidis, 1997). The geostatistical analyses and interpolation were realized by spatial geostatistical analysis tools in ARCGIS10.1.

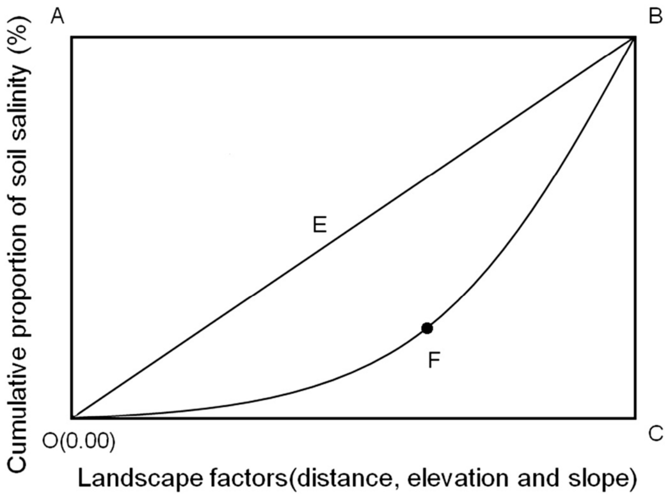

Fig. 2. The Lorenz curve as applied to soil salinity accumulation (SSA) across a watershed. O refers the soil sample near the outlet of the studied watershed. X-axis refers landscape factors, Y-axis refers the cumulative proportion of the total soil salinity accumulation index with increasing landscape factors such as distance, relative elevation, and slope. Cutoff point (F) is shown as black circle on the Lorenz curves. OEB indicating perfect equality of soil salinity accumulation and migration is shown for reference.

We used the Eq. (3) to quantify the soil salt accumulation state among regions and land use types and used the distribution of soil salt content to estimate the quantity of SSA in individual regions and land use types (Wang and Li, 2013). For each individual land use type with k patches, we calculated the amount of SSA using the following Eq. (3):

$$SSA_d = \sum_{i=1}^{k} SSA_i = \sum_{i=1}^{k} \rho_i \times S_i \times D_i \times (1-V_i) \times A_i \quad (3)$$

where SSA_i refers the quantity of salt accumulation in soil (g), ρ_i refers the bulk density (Mg/m^3), S_i refers the distribution area (m^2) in degree of soil salt content i, D_i refers the soil thickness (m), V_i refers the volume fraction of fragments >2 mm and A_i the mean value of soil salt content (g/kg^{-1}). The statistical difference in SSA of the same land use type between 1982 and 2015 was analyzed using independent-samples t-test in SPSS20.0a.

2.4. Using the Lorenz curve to identify the SSA process

The Lorenz curve is usually used to indicate social inequality, and was original by economists (Chakravarty, 1990; Lorenz, 1905). It is successful applied in the fields of environment and ecology (Abell et al., 2013; Shi et al., 2013), and regarded as an active area of research for the Lorenz curve to develop new functional forms (Ogwang and Rao, 1996). In the space of a watershed, when the outlet is selected as the reference point, the source and sink landscapes pattern is identified by comparing them with the landscape properties, such as relative distance, relative elevation and relative slope gradient from outlet of the river to the sampling point (Chen et al., 2009). In this study, the site of the southernmost sampling point nearby the watershed outlet was selected as the reference point because of salinity transported from the upstream to the downstream watershed (Wang and Li, 2010). In the study area, the elevation of landform is a major cause for the spatial variability of soil salinity in the space of watershed (Wang et al., 2008a). The Lorenz curves were constructed to determine how the cumulative proportion of the total soil salinity accumulation index (SI) that varies with respect to the spatial landscape factors (e.g. distance and relative elevation) (Fig. 2). The SI was calculated as follows:

$$\mathrm{SI_n} = [(SP_i - MP) + (SP_{i+1} - MP) + \cdots\cdots + (SP_n - MP)] / \sum_{i=0}^{n} (SP_i - MP) \quad (4)$$

where SP_i is the soil salt content at sampling point i in the study area; MP represents soil salt content as the reference point of the outlet in the watershed and $\mathrm{SI_n}$ is the value of soil salinity accumulation from the referent point to point n.

The measure of inequality of Lorenz curve is indicated by the Gini coefficient (G). In this study, the G was used to quantify inequality of the total soil salinity accumulation index (SI) with increasing landscape factors such as relative distance, relative elevation, and relative slope. The G varies from 0 to 1, with 0 implying soil salinity being constant in an entire watershed and 1 implying soil salinity at the maximum value of landscape factors. This parameter is calculated by the ratio of two areas. The area in nominate is enclosed by the Lorenz curve and the line of perfect equality of soil salinity accumulation and migration. The denominate is the area under the line of perfect equality of soil salinity migration and accumulation (Fig. 2). Cutoff point of G refers to the point on the Lorenz curve, where the distance between perfect equality line and the Lorenz curve is longest (Fig. 2). The G was calculated as follow: enclose

$$G = 1\text{-}2 \int_0^1 Y(X) dX \quad (5)$$

where $Y(X)$ is Lorenz curve, and X is a distribution of standardized cumulative to the standardized SI.

3. Results

3.1. Descriptive statistics for soil salt content in the watershed

The mean value of soil salt content in 1982 (5.91 g/kg) was non-significantly higher than in 2015 (5.27 g/kg, $p > 0.05$, Table 1); the corresponding ranges were 0.40–23.8 and 0.24–33.18 g/kg. The mean soil salt content decreased by 10.8% during 1982–2015. The values of CV were >1, indicating that salt content of the surface soil varied greatly in the study area. The K–S test showed that soil salt content in both 1982 and 2015 followed the normal distribution (Table 1, $p < 0.05$), indicating that the data were appropriate for the geostatistical analysis using a semi-variogram (Li and Reynolds, 1995).

According to the variogram analysis, the soil salt content in both 1982 and 2015 followed the exponential pattern (Table S1). The values of the determining coefficient (R^2) were >0.6; the residual sum of squares (RSS) was close to zero (0.0005 in 1982 and 0.0004 in 2015) and the F-tests for R^2 were significant at $\alpha = 0.01$ level (Table S1, $p < 0.01$). These parameters showed that the exponential models well represented the spatial pattern of the soil salt content. The nugget (C0) and sill (C0 + C) usually are used to reflect spatial heterogeneity of soil elements (Cambardella et al., 1994). The ratio of nugget and sill (C0/C0 + C) in the nugget variance can express the total spatial heterogeneity. The C0/C0 + C) in 1982 and 2015 were <0.25, suggesting strong spatial autocorrelation between salt content in the watershed (Chien et al.,

Table 1
Summary statistics and K–S test for soil salt content.

Time	Sample size	Mean	SD	Coefficient of variation	Max.	Min.	Skewness	Kurtosis	K–S test
1982	145	5.91	6.22	1.05	23.8	0.40	1.48	1.02	2.56
2015	290	5.27	7.35	1.40	33.1	0.24	1.95	3.25	4.58

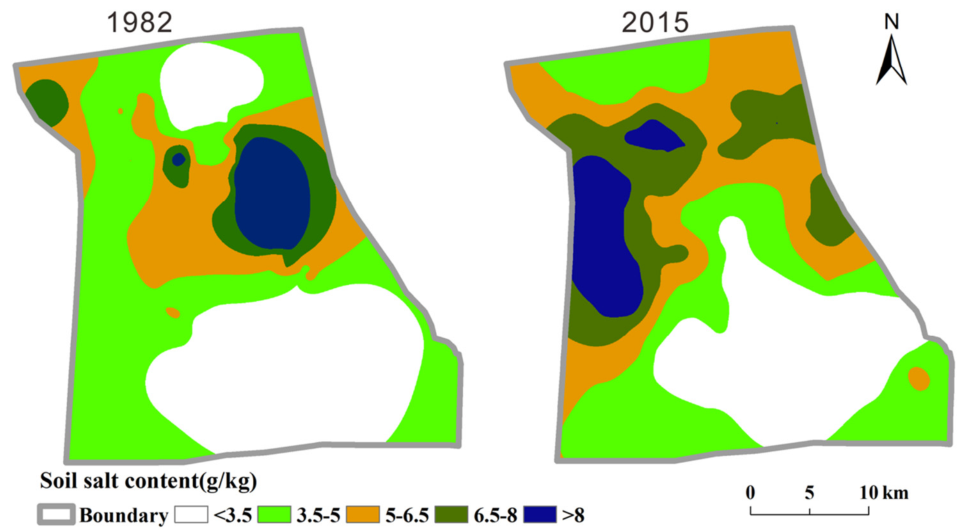

Fig. 3. The spatial distribution of salt content in the top 20 cm soils in 1982 and 2015.

1997). For the spatial prediction of salt content in soil, the standardized ME of predictions was very small (0.005 in 1982 and −0.0004 in 2015), and the RMSSE ranged from 0.908 to 1.084 (Table S1), demonstrating that the spatial maps of salt content in 1982 and 2015 estimated by ordinary kriging interpolation were reliable and acceptable (Kitanidis, 1997).

3.2. Distribution of soil salt content during 1982–2015

When the soil salt content is lower than 3.5 g/kg in this region, there is little effect on crop production (Xinjiang Institute of Desert and Soil Chinese Academic Sciences, 2000). So, soil salt content in this study was divided into five classes: <3.5, 3.5–5.0, 5.0–6.5, 6.5–8.0 and >8.0 g/kg (Fig. 3). Soil salt content generally increased from the south to the center of the region, with low soil salt contents in the south and high soil salt contents in the middle region of the watershed. Soil salt contents were clearly correlated with the land use change. There were significantly different soil salt content patterns during 1982–2015 in the study area (Fig. 3). There was also considerable change in the study area during 1982–2015, and approximately 56% of the total area experienced transitional changes (Table 2) – notably areas of soil salt content of 3.5–5.0 g/kg (decreased by 8678 ha, about 23%) and 6.5–8.0 g/kg (increased by 8342 ha, about 2.41 times). The area of soil salt content <5.0 g/kg was reduced from 68,080 ha in 1982 to 51,483 ha in 2015. Clearly, the area of soil salinization considerably increased as the degree of soil salt content did. Compared to 1982, the area of soil salt content of 5.0–6.5 g/kg increased by 40.9% and the area of soil salt content >8.0 g/kg increased by 40.6% in 2015. However, the increases in area of soil salt content >8.0 g/kg was small – only 2094 ha. These results could show an accelerated trend of soil salinization.

Table 2
Transition matrix of area (ha) of different soil salt contents during 1982–2015.

1982	Soil salt content in 2015 (g/kg)					
	<3.5	3.5–5	5–6.5	6.5–8	>8	Sum
<3.5	20,234	7880	2606	459	0	31,178
3.5–5	1848	14,710	8818	5493	6031	36,900
5–6.5	524	2512	4887	5988	1142	15,053
6.5–8	425	895	2681	1845	77	5925
>8	226	2227	2221	483	0.27	5157
Sum	23,259	28,223	21,214	14,267	7251	94,215

3.3. The Lorenz curve and Gini coefficient concerning SI

The values of R^2 for Lorenz curves of SI for relative distance and relative elevation in 1982 and 2015 were showed in Fig. 4, respectively. All the values were significantly higher than 0.80 (0.99 and 0.84 for relative distance and for relative elevation in 1982, respectively, and 0.99 and 0.91 in 2015; Fig. 4, $p < 0.01$), indicating that these curves well represented the distribution of SI in relation to relative distance and relative elevation change. Levels of inequality, measured by Gini coefficients, were similar for relative distance and elevation in the 1982 and 2015 datasets. Values for the Gini coefficient were higher for both distance and elevation in 1982 than in 2015 (0.34 and 0.22 for relative distance in 1982, respectively, and 0.61 and 0.53 for relative elevation in 2015; Fig. 4), which showed that regions of soil salinity migration or accumulation were not equal during 1982–2015. Thus, locations of the cutoff point in Lorenz curves would be closer to 0 in 1982 than in 2015. This information suggests that land use changes play an import role in soil salinity accumulation during 1982–2015. At the same time, Fig. 3 shows that the center of gravity of salinity may have moved to the west of the study area. It seems that so have croplands (Fig. S1). This showed again that land use can cause soil salt content change. The boundaries of soil salinity migration and accumulation at the watershed scale were identified as cutoff points for relative distance and elevation in 1982 and 2015. Location of cutoff points for relative distance and relative elevation to the outlet were 12.37 km and −120.6 m in 1982 (Fig. 4), respectively, indicating soil salinity migration in the region of 0–12.37 km for relative distance and −120.6 to 0 m for relative elevation. For 2015, there were similar characteristics to those in 1982, with soil salinity migration in the region of 0–11.07 km for relative distance and −114.9 to 0 m for relative elevation (Fig. 4). During 1982–2015, the location of cutoff points correlated with the distance and elevation tended to be near the reference point of the outlet in the watershed, suggesting that the area of the region of soil salinity migration was reducing but the region of soil salinity accumulation was expanding. Soil salinity migration occurred in the south of the watershed, but the accumulation in the north. This means that soil salinity transport was in the upstream watershed and soil salinity accumulation was in the downstream watershed.

3.4. Change of SSA in migration and accumulation regions during 1982–2015

The change of SSA in the 0–20 cm depth in different regions during 1982–2015 is shown in Fig. 5. There was a remarkable change in SSA between migration and accumulation regions, with clear differences in

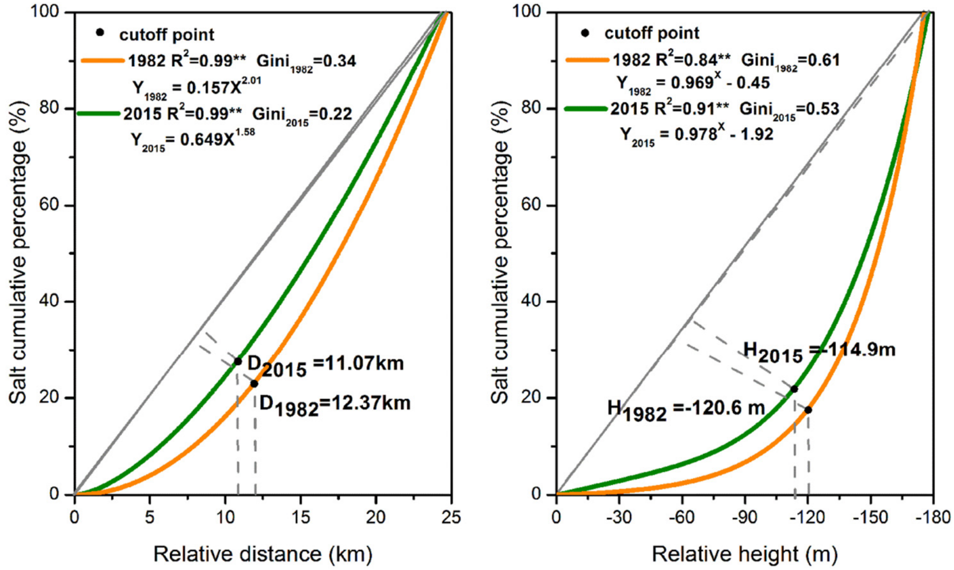

Fig. 4. Lorenz distribution curves of SI by area-accumulated percentage both in 1982 and 2015.

SSA per unit area between the two regions (Fig. 5, $p < 0.01$). Additionally, SSA per unit area was significantly lower in the migration than the accumulation region (Fig. 5, $p < 0.01$). SSA per unit area for the migration region increased from 0.70 to 0.87 kg/m^2 during 1982–2015, and correspondingly from 1.55 to 1.87 kg/m^2 for the accumulation region. Regardless of migration or accumulation region, the mean of SSA value was larger in 2015 than 1982 ($p < 0.01$) and the value increased by over 16% in per unit area during 1982–2015, indicating that the process of soil salinization was accelerating in the study area.

3.5. SSA in land use types during 1982–2015

The mean SSA of the six main landscape types varied from 0.81 kg/m^2 for grassland to 1.82 kg/m^2 for planted forest (Fig. 6). In the entire watershed, relative to 1982 levels, SSA per unit area increased by 0.32 kg/m^2 in cropland, 0.31 kg/m^2 in planted forest, 0.25 kg/m^2 in grassland, 0.13 kg/m^2 in shrub land, 0.35 kg/m^2 in sandy desert and 0.35 kg/m^2 in salinized land in 2015 – accounting for 33.68, 20.53, 30.86, 9.15, 31.53 and 31.53% of 1982 values, respectively (Fig. 6). The rate of SSA per unit area increase in cropland was highest among the various landscape types during 1982–2015. The SSA per unit area was higher in planted forest than any other landscape type in 1982 and 2015, but the SSA per unit area of cropland increased most rapidly over this period.

Comparing the SSA per unit area with artificial and natural landscapes for the same period showed that the increasing intensity of SSA per unit area was significant in both irrigated and non-irrigated landscapes during 1982–2015 (Fig. 7). The SSA per unit area in irrigated land was <0.75 kg/m^2 in the migration region, but >1.4 kg/m^2 in the accumulation region. Similarly, The SSA per unit area in non-irrigated land was <0.96 kg/m^2 in the migration region, but >1.59 kg/m^2 in the accumulation region. In both 1982 and 2015, the SSA per unit area was 0.06–0.22 kg/m^2 higher for non-irrigated than irrigated land. The increase in the SSA per unit area during 1982–2015 varied from 0.45 kg/m^2 in irrigated land to 0.17 kg/m^2 in non-irrigated land (more than double) (Fig. 7). However, the SSA per unit area differed considerably between the migration and accumulation regions (Fig. 7). In the migration region, relative to 1982 levels, SSA per unit area increased by 0.1 kg/m^2 in irrigated and 0.23 kg/m^2 in non-irrigated land. During the same period, in the accumulation region, the corresponding SSA per unit area increased by 0.29 and 0.17 kg/m^2. The conversion of natural landscape to crop land in arid areas clearly affected SSA per unit area changes in time and space.

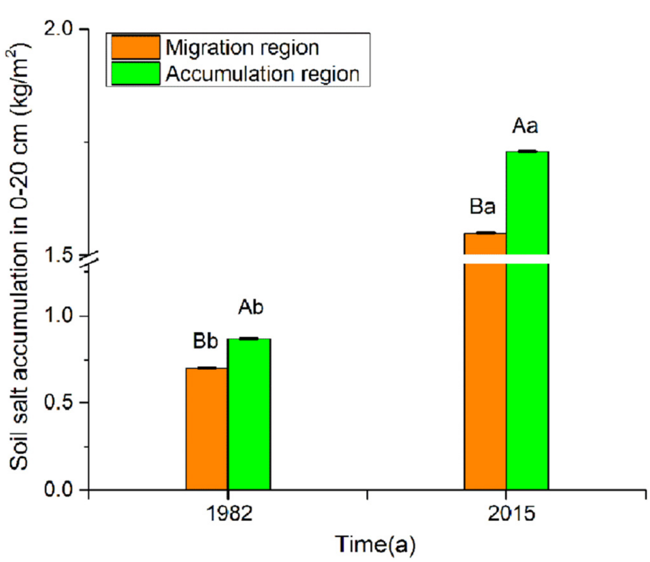

Fig. 5. SSA in the top 20 cm soils for migration and migration regions in the study area.

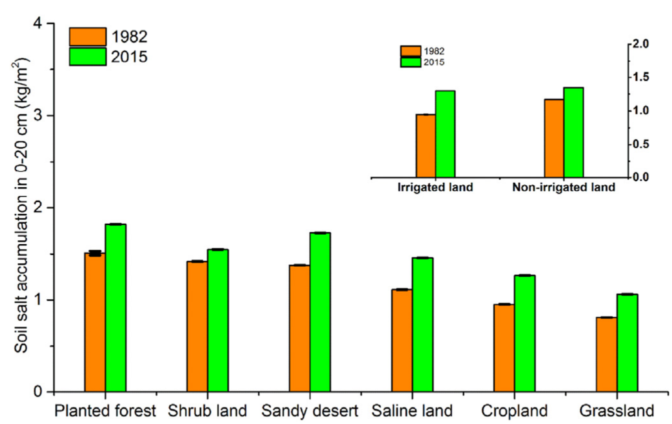

Fig. 6. SSA in the top 20 cm soils for various landscape types in the study area.

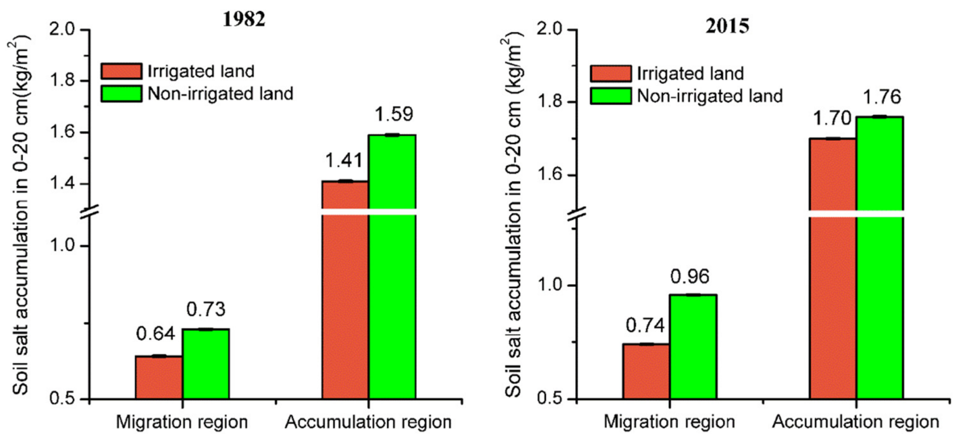

Fig. 7. SSA in the top 20 cm soils for irrigated and non-irrigated land in migration and accumulation regions of the study area.

4. Discussion

4.1. Spatial variation of soil salinity in the watershed

The spatial variation of soil salinity is generally great, and its average levels often reflect topography (Utset and Borroto, 2001). Our data suggested that salt content in the surface soil of the studied area varied greatly at the watershed scale in 1982 and 2015 (Table 1). Water in soil is the key driver for soil salinity transport and change. Environmental factors such as topography, climate and hydrological conditions can directly affect water movement in soil, and promote the exchange of salt ions in soil solution (Utset and Borroto, 2001). In our study area, elevation was the primary factor affecting spatial variation of soil salt content (Fig. 1) (Wang et al., 2008a). The elevation difference is up to 180 m. Furthermore, changes of land use could relatively rapidly affect the salt content by altering the infiltration rate (Fang et al., 2005). The study region has experienced severe soil salinization after land use change in the past 30 years (Fig. S1 and Fig. 3). During 1982–2015, human activities and land reclamation has converted transformed natural landscape into planted and cultivated landscape, with an increase in irrigated cropland (Fig. S1). These changes to irrigated land may be the cause of the higher CV of soil salt content in 2015 than in 1982 (Table 1), which generally has strong spatial dependence in topsoil (Liu et al., 2016; Cemek et al., 2007). The spatial variations of soil salinity might be resulted by the impacts of human activities on soil processes in the region (Wang et al., 2008a). Thus, robust spatial autocorrelation of salt content in soil showed that its spatial dependence was primarily caused by structural factors (Table S1).

Spatial changes in soil salt content could be due to the impacts of environmental changes and human activities on soil processes, such as crop sequences, agricultural irrigation, fertilizer, groundwater table change, evaporation and precipitation (Bargaz et al., 2016; Wang et al., 2008b). Spatial analyses showed that about 56% of studied area had experienced changes in the degree of soil salt content during 1982–2015 (Table 2). Extremely likely changes occurred in 11.07% of areas with soil salt content > 6.5 g/kg, and significant and intense soil salinity accumulation was shown in the whole study area, especially in the lower watershed (Fig. 3). The accumulation of soil salinity in irrigated cropland is the result of water loss through evapotranspiration which increases concentrations of salts in the remaining water (Wichelns and Qadir, 2015). Since the area of cropland has expanded remarkably which requires more water for irrigation in the Sangong River watershed, the groundwater table and degree of groundwater mineralization in the entire watershed have increased substantially, especially in the lower part of the study area (Wang and Li, 2013), which has directly led to soil salinization and the resultant higher evapotranspiration (Han et al., 2011; Qadir et al., 2001).

4.2. The migration and accumulation regions of soil salinity across the watershed

In this watershed, soil salt tends to be transported downward from mountainous areas to the alluvial plains by snowmelt and surface and sub-surface run-off and accumulates in the lower part (Wang and Li, 2013).Salinity was low in higher landscape positions in alluvial fans of the watershed (Fig. S1 and Fig. 3) and in well drained soils that has coarser soil texture (Metternicht, 2001). However, it is usually not clear where the boundary lies between the migration and accumulation regions. For this reason, we applied the methodology of the Lorenz curve to distinguish between migration and accumulation regions using the extensive data on soil salt content in the watershed, using limited parameter data for SI, and then addressed the characteristics of soil salinity accumulation both in migration and accumulation regions. An important requisite of the Lorenz curve approach is that the locations of the soil salinity calibration sites for SI should first be ascertained as representative values of soil salt content to compare with the reference point of the outlet in the entire survey region. The Lorenz curve indicated that a sink landscape was present in the top 0–20 cm soil in the Sangong River watershed (Chen et al., 2009). Lorenz curves describing the proportions of soil salinity accumulation showed that the boundary between soil salinity migration and accumulation regions was lower in 2015 than in 1982 (Fig. 4), suggesting a spatio-temporal inequality in loading of the soil salinity transport region. This indicated a significant process of soil salinity migration from the upper to the lower study area during 1982–2015. Thus, the change in SSA per unit during 1982–2015 in the migration region was no significantly different from that in the accumulation region (Fig. 5, $p < 0.05$). It is clear that there is a tradeoff location for the migration and accumulation regions in the watershed. These data suggest that cutoff points for Lorenz curves would determine the boundary of regions of migration and accumulation at the watershed scale. So, Lorenz curves were an appropriate method to identify the region between soil salinity migration and accumulation at the watershed scale.

4.3. Impact of land use change on SSA

Land use type has been shown to be a critical controller of soil ions status and movement at the watershed scale (Wang et al., 2009). Farmland is the major part of inland basins in northwest of China, and their changes are the key of sustainable development of agriculture (Wahap et al., 2004). Human activities are the most important contributor for the changes in agricultural landscape patterns (Fu et al., 2006). The impacts of landscape pattern change on soil salinity are complex and differ among land use types at different landscape scales (Daliakopoulos et al., 2016). During 1982–2015, farmland dominated land use types in the

Sangong River watershed, and land use change showed increasing multiplicity and fragmentation (Fig. S1). The changes of land use patterns also significantly affect the migration and accumulation of soil salt ions (Fang et al., 2005; Tuteja et al., 2003). Farmland exploitation significantly affects soil properties (Li and Shao, 2014; Jia et al., 2011; Sveistrup et al., 2005), leading to variations in salt accumulation in soil among land use types (Fig. 6).

Accurate spatial information concerning small changes in soil salinity levels is important for many agronomic practices, such as fertilizer, crop selection, tillage and irrigation. Appropriate agricultural practices can improve soil quality to ameliorate salt accumulation in soil. These practices include the appropriate crop covering, the plantation of salt tolerance plant, the compost supplemented with trichoderma harzianum (Mbarki et al., 2017; Yan et al., 2013). Arid areas are characteristic of saline or alkaline soil and high evapotranspiration with low precipitation. In this condition, over irrigation is proved to be an efficient approach to control soil salinity in the process of agriculture production Li H.Y. et al., 2015; Li Y. et al., 2015). Agricultural and planted forest irrigation through the construction of ditches could induce water imbalances at a regional level, and lead to great spatial variations of soil salinity (Yu et al., 2009; Ritzema et al., 2008). Thus, over the last 30 years, soil salinization due to human activities has been intensified in the study area, especially in irrigated land (Fig. 7). The amount of land coverage affects the evaporation and soil salt content in the surface layer (Sun et al., 2011). Regardless of migration or accumulation region, the SSA per unit increased for all land use types, indicating a process of soil salinization due to land use conversion. Indeed, natural factors (such as climate) in arid zones can cause salt accumulation in surface soil. It is challenging to accurately quantify the contribution of natural and human factors influencing salt accumulation in soil under various landscape changes for large spatial extents. Due to the complex relationship of soil salinity with soil water, the currently available information concerning salt accumulation for inland basins is insufficient to determine the contribution of salt accumulation at different landscape scales from the change in a single land use type. In this study, we only focused on soil salinity at the depth of top 20 cm. This didn't reflect the soil salinity transport throughout soil profile. Future research should introduce more variables to the variogram/kriging application to address salt accumulation along soil profile at watershed scale.

5. Concluding remarks

Few studies have specifically addressed the issue of spatial change for soil salinity accumulation at the watershed scale. Soil salinization is a main issue for agricultural sustainability in China. This study examined the spatio-temporal patterns of soil salinity accumulation of various land use types in a typical watershed, which is located in an arid area of northwest China. We found greater soil salinity accumulation in the surface layers of all land use types in the Sangong River watershed during 1982–2015. About 56% of the studied area experienced transition the degree of soil salt content from one class to another. Lorenz curves describing the proportions of soil salinity accumulation showed a spatio-temporal inequality in loading of the soil salinity transport region. Thus, the boundaries of salt migration and transport areas were identified in this study. The dramatic accumulation of soil salinity in all land use types was obvious in the agricultural watershed of this arid region. The Lorenz curves and geostatistical analyses of soil salinity advance our understanding of the spatio-temporal variations of soil salinization in the long-term process of land use at the watershed scale. This is a valuable way to identify the spatial regional change in soil salinity accumulation. This study provides an insight into the spatial patterns of soil salinity accumulation, which is especially useful for estimating the region of spatial transport of soil salinity at the watershed scale. According to the pattern of soil salinity accumulation under various land use types in the watershed space, the spatial pattern of soil salinity will help select reasonable utilization of agricultural water resources for efficient management in environments that are regulated by salt. Therefore, this information will be helpful for providing guidelines in agricultural land use and so controlling soil salinization in arid land.

Acknowledgments

This work were financially supported by the Xinjiang Province Outstanding Youth Talent Project (No. 2014711009), the National Natural Science Foundation of China (No. 41371200 and No. 41501205) and the 'Western Light' program of the Chinese Academy of Sciences (No. 2015-XBQN-A-06).

Appendix A. Supplementary data

Supplementary data to this article can be found online at https://doi.org/10.1016/j.scitotenv.2017.11.222.

References

Abell, J.M., Hamilton, D.P., Rutherford, J.C., 2013. Quantifying temporal and spatial variations in sediment, nitrogen and phosphorus transport in stream inflows to a large eutrophic lake. Environ. Sci. Proc. Imp. 15 (6), 1137–1152.
Abliz, A., Tiyip, T., Ghulam, A., Halik, Ü., Ding, J.L., Sawut, M., et al., 2016. Effects of shallow groundwater table and salinity on soil salt dynamics in the Keriya Oasis, Northwestern China. Environ. Earth Sci. 75 (3), 260.
Amundson, R., Berhe, A.A., Hopmans, J.W., Olson, C., Sztein, A.E., Sparks, D.L., 2015. Soil and human security in the 21st century. Science 348, 1261071.
Aragüés, R., Medina, E.T., Zribi, W., Clavería, I., Álvaro-Fuentes, J., Faci, J., 2014. Soil salinization as a threat to the sustainability of deficit irrigation under present and expected climate change scenarios. Irrig. Sci. 33, 67–79.
Bao, S.D., 2000. Soil and Agricultural Chemistry Analysis. Chinese Agricultural Press, Beijing, pp. 178–198.
Bargaz, A., Nassar, R.M.A., Rady, M.M., Gaballah, M.S., Thompson, S.M., Brestic, M., et al., 2016. Improved salinity tolerance by phosphorus fertilizer in two phaseolus vulgaris recombinant inbred lines contrasting in their p-efficiency. J. Agron. Crop Sci. 202, 497–507.
Beltran, J.M., 1999. Irrigation with saline water: benefits and environmental impact. Agric. Water Manag. 40, 183–194.
Bennett, L.T., Mele, P.M., Annett, S., Kasel, S., 2010. Examining links between soil management, soil health, and public benefits in agricultural landscapes: an Australian perspective. Agric. Ecosyst. Environ. 139, 1–12.
Benyamini, Y., Mirlas, V., Marish, S., Gottesman, M., Fizik, E., Agassi, M., 2005. A survey of soil salinity and groundwater level control systems in irrigated fields in the Jezre'el Valley, Israel. Agric. Water Manag. 76 (3), 181–194.
Bui, E.N., 2013. Soil salinity: a neglected factor in plant ecology and biogeography. J. Arid Environ. 92, 14–25.
Butcher, K., Wick, A.F., DeSutter, T., Chatterjee, A., Harmon, J., 2016. Soil salinity: a threat to global food security. Agron. J. 108, 2189–2200.
Cambardella, C.A., Moorman, T.B., Novak, J.M., Parkin, T.B., Karlen, D.L., Turco, R.F., Konopka, A.E., 1994. Field-scale variability of soil properties in central Iowa soils. Soil Sci. Soc. Am. J. 58, 1501–1511.
Cassel, F., Goorahoo, D., Sharmasarkar, S., 2015. Salinization and yield potential of a salt-laden Californian soil: an in situ geophysical analysis. Water Air Soil Pollut. 226, 422.
Castrignano, A., Maiorana, M., Fornaro, F., Lopez, N., 2002. 3D spatial variability of soil strength and its change over time in a durum wheat field in southern Italy. Soil Tillage Res. 65, 95–108.
Cemek, B., Guler, M., Kilic, K., Demir, Y., Arslan, H., 2007. Assessment of spatial variability in some soil properties as related to soil salinity and alkalinity in Bafra plain in northern Turkey. Environ. Monit. Assess. 124 (1–3), 223–234.
Cetin, M., Kirda, C., 2003. Spatial and temporal changes of soil salinity in a cotton field irrigated with low-quality water. J. Hydrol. 272, 238–249.
Chakravarty, S.R., 1990. Ethical Social Index Numbers. Springer-Verlag, New York.
Chen, L., Tian, H., Fu, B., Zhao, X., 2009. Development of a new index for integrating landscape patterns with ecological processes at watershed scale. Chin. Geogr. Sci. 19, 37–45.
Chien, Y.J., Lee, D.Y., Guo, H.Y., Houng, K.H., 1997. Geostatistical analysis of soil properties of mid-west Taiwan soils. Soil Sci. 162, 291–297.
Corwin, D.L., Lesch, S.M., Oster, J.D., Kaffka, S.R., 2006. Monitoring management-induced spatio-temporal changes in soil quality through soil sampling directed by apparent electrical conduction. Geoderma 131, 369–387.
Cruz-Cárdenas, G.L., 2014. Interpolation of Mexican soil properties at a scale of 1: 1,000,000. Geoderma 213, 29–35.
Daliakopoulos, I.N., Tsanis, I.K., Koutroulis, A., Kourgialas, N.N., Varouchakis, A.E., 2016. The treat of soil salinity: a European scale review. Sci. Total Environ. 573, 727–739.
Devkota, M., Gupta, R.K., Martius, C., Lamers, J.P.A., Devkota, K.P., Sayre, K.D., Vlek, P.L.G., 2015. Soil salinity management on raised beds with different furrow irrigation modes in salt-affected lands. Agric. Water Manag. 152, 243–250.
Ding, J.L., Wu, M.C., Tiyip, T., 2011. Study on soil salinization information in arid region using remote sensing technique. Agric. Sci. China 10, 404–411.

Douaik, A., Meirvenne, M.V., Tóth, T., 2005. Soil salinity mapping using spatio-temporal kriging and Bayesian maximum entropy with interval soft data. Geoderma 128 (3), 234–248.
Fang, H.L., Liu, G.H., Kearney, M., 2005. Georelation analysis of soil type, soil salt content, landform, and land use in the Yellow River delta. Environ. Manag. 35, 72–83.
Fernandez-Buces, N., Siebe, C., Cram, S., Palacio, J.L., 2006. Mapping soil salinity using a combined spectral response index for bare soil and vegetation: a case study in the former lake Texcoco, Mexico. J. Arid Environ. 65, 644–667.
Foley, J.A., Ramankutty, N., Brauman, K.A., Cassidy, E.S., Gerber, J.S., Johnston, M., et al., 2011. Solutions for a cultivated planet. Nature 478, 337.
Fu, B., Hu, C., Chen, L., Hommay, O., Gulinck, H., 2006. Evaluating change in agricultural landscape pattern between 1980 and 2000 in the Loess hilly region of Ansai County, China. Agric. Ecosyst. Environ. 114, 387–396.
Fukang Land Resource Administration, 1983. Land Use and Soil Inventory Report in 1982.
Fukang Land Resource Administration, 2015. Land Use Maps in 1982 and 2015.
Ghassemi, F., Close, A., Kellett, J.R., 1997. Numerical models for the management of land and water resources salinisation. Math. Comput. Simul. 43, 323–329.
Goovaerts, P., 1999. Geostatistics in soil science: state-of-the-art and perspectives. Geoderma 89, 1–45.
Han, D., Song, X., Currell, M.J., Cao, G., Zhang, Y., Kang, Y., 2011. A survey of groundwater levels and hydrogeochemistry in irrigated fields in the Karamay Agricultural Development Area, northwest China: implications for soil and groundwater salinity resulting from surface water transfer for irrigation. J. Hydrol. 405, 217–234.
Herrero, J., Pérez-Coveta, O., 2005. Soil salinity changes over 24 years in a Mediterranean irrigated district. Geoderma 125, 287–308.
Ibrakhimov, M., Martius, C., Lamers, J.P.A., Tischbein, B., 2011. The dynamics of groundwater table and salinity over 17 years in Khorezm. Agric. Water Manag. 101, 52–61.
Jalila, J., Moncef, B., Hatem, E., 2016. Salt removal from soil using the argil porous ceramic. Desalination 379, 53–67.
Jia, S.H., Zhou, D., Xu, D.Z., 2011. The temporal and spatial variability of soil properties in an agricultural systems as affected by farming practices in the past 25 years. J. Food Agr. Environ. 9, 669–676.
Juan, P., Mateu, J., Jordan, M.M., Mataix-Solera, J., Meléndez-Pastor, I., Navarro-Pedreño, J., 2011. Geostatistical methods to identify and map spatial variations of soil salinity. J. Geochem. Explor. 108 (1), 62–72.
Kitanidis, P.K., 1997. Introduction to Geostatistics: Applications in Hydrogeology. Cambridge University Press, Cambridge, UK.
Lal, R., 2015. Restoring soil quality to mitigate soil degradation. Sustainability 7, 5875–5895.
Li, H., Reynolds, J.F., 1995. On definition and quantification of heterogeneity. Oikos 73, 280–284.
Li, D., Shao, M., 2014. Soil organic carbon and influencing factors in different landscapes in an arid region of northwestern China. Catena 116, 95–104.
Li, J.G., Pu, L.J., Han, M.F., Zhu, M., Zhang, R.S., Xiang, Y.Z., 2014. Soil salinization research in China: advances and prospects. J. Geogr. Sci. 24, 943–960.
Li, H.Y., Webster, R., Shi, Z., 2015a. Mapping soil salinity in the Yangtze delta: REML and universal kriging (E-BLUP) revisited. Geoderma 237, 71–77.
Li, Y., Wang, Y., Houghton, R.A., Tang, L., 2015b. Hidden carbon sink beneath desert. Geophys. Res. Lett. 42, 5880–5887.
Liu, G., Li, J., Zhang, X., Wang, X., Lv, Z., Yang, J., et al., 2016. GIS-mapping spatial distribution of soil salinity for eco-restoring the yellow river delta in combination with electromagnetic induction. Ecol. Eng. 94, 306–314.
Lorenz, M.O., 1905. Methods for measuring the concentration of wealth. J. Am. Stat. Assoc. 9, 209–219.
Mbarki, S., Cerdà, A., Brestic, M., Mahendra, R., Abdelly, C., Pascual, J.A., 2017. Vineyard compost supplemented with trichoderma harzianum t78 improve saline soil quality. Land Degrad. Dev. 28, 1028–1037.
Metternicht, G., 2001. Assessing temporal and spatial changes of salinity using fuzzy logic, remote sensing and GIS. Foundations of an expert system. Ecol. Model. 144, 163–179.
Monestiez, P., Allard, D., Froidevaux, R., 2010. Geoenv iii — geostatistics for environmental applications. Quant. Geol. Geostat. 36 (44), 3251–3256.
Niñerola, V.B., Navarro-Pedreño, J., Lucas, I.G., Pastor, I.M., Vidal, M.M.J., 2017. Geostatistical assessment of soil salinity and cropping systems used as soil phytoremediation strategy. J. Geochem. Explor. 174, 53–58.
Nurmemet, I., Ghulam, A., Tiyip, T., Elkadiri, R., Ding, J.L., Maimaitiyiming, M., et al., 2015. Monitoring soil salinization in Keriya River Basin, northwestern China using passive reflective and active microwave remote sensing data. Remote Sens. 7, 8803–8829.
Ogwang, T., Rao, U.L.G., 1996. A new functional form for approximating the Lorenz curve. Econ. Lett. 52, 21–29.
Pankova, E.I., Aidarov, I.P., Golovanov, D.L., Yamnova, I.A., 2015. Salinization as the main soil-forming process in soils of natural oases in the Gobi desert. Eurasian Soil Sci. 48, 1017–1028.
Pozdnyakova, L., Zhang, R.D., 1999. Geostatistical analyses of soil salinity in a large field. Precis. Agric. 1, 153–165.
Preston, S.D., Bierman Jr., V.J., Silliman, S.E., 1989. An evaluation of methods for the estimation of tributary mass loads. Water Resour. Res. 25 (6), 1379–1389.
Qadir, M., Oster, J.D., 2004. Crop and irrigation management strategies for saline-sodic soils and waters aimed at environmentally sustainable agriculture. Sci. Total Environ. 323, 1–19.
Qadir, M., Ghafoor, A., Murtaza, G., 2001. Amelioration strategies for saline soils: a review. Land Degrad. Dev. 11, 501–521.
Renard, P., Demougeot-Renard, H., Froidevaux, R., 2005. Geostatistics for environmental applications. Proceedings of the Fifth European Conference on Geostatistics for Environmental Applications. Springer Berlin Heidelberg, New York.
Rengasamy, P., 2006. World salinization with emphasis on Australia. J. Exp. Bot. 57, 1017–1023.
Ritzema, H.P., Satyanarayana, T.V., Raman, S., Boonstra, J., 2008. Subsurface drainage to combat waterlogging and salinity in irrigated lands in India: lessons learned in farmers' fields. Agric. Water Manag. 95, 179–189.
Salvati, L., Ferrara, C., 2015. The local-scale impact of soil salinization on the socioeconomic context: an exploratory analysis in Italy. Catena 127, 312–322.
Scudiero, E., Skaggs, T.H., Corwin, D., 2016. Comparative regional-scale soil salinity assessment with near-ground apparent electrical conductivity and remote sensing canopy reflectance. Ecol. Indic. 70, 276–284.
Scudiero, E., Skaggs, T.H., Corwin, D., 2017. Simplifying field-scale assessment of spatiotemporal change of soil salinity. Sci. Total Environ. 587–588, 273–278.
Sheng, J., Ma, L., Jiang, P., Li, B., Huang, F., Wu, H., 2010. Digital soil mapping to enable classification of the salt-affected soils in desert agro-ecological zones. Agric. Water Manag. 97, 1944–1951.
Shi, W., Yu, X., Liao, W., Wang, Y., Jia, B., 2013. Spatial and temporal variability of daily precipitation concentration in the Lancang River basin, China. J. Hydrol. 495, 197–207.
Singh, A., 2015. Soil salinization and waterlogging: a threat to environment and agricultural sustainability. Ecol. Indic. 57, 128–130.
Sun, Y., Li, X., Mander, U., He, Y., Jia, Y., Ma, Z., et al., 2011. Effect of reclamation time and land use on soil properties in Changjiang River Estuary. Chin. Geogr. Sci. 21, 403–416.
Sveistrup, T.E., Haraldsen, T.K., Langohr, R., Marcelino, V., Kværner, J., 2005. Impact of land use and seasonal freezing on morphological and physical properties of silty Norwegian soils. Soil Tillage Res. 81, 39–56.
Taghizadeh-Mehrjardi, R., Minasny, B., Sarmadian, F., Malone, B.P., 2014. Digital mapping of soil salinity in Ardakan region, central Iran. Geoderma 213, 15–28.
Tripathi, R., Nayak, A.K., Shahid, M., Raja, R., Panda, B.B., Mohanty, S., et al., 2015. Characterizing spatial variability of soil properties in salt affected coastal India using geostatistics and kriging. Arab. J. Geosci. 8, 10693–10703.
Tuteja, N.K., Beale, G., Dawes, W., Vaze, J., 2003. Predicting the effects of land use change on water and salt balance-a case study of a catchment affected by dryland salinity in NSW, Australia. J. Hydrol. 283 (1), 67–90.
Utset, A., Borroto, M., 2001. A modeling-GIS approach for assessing irrigation effects on soil salinisation under global warming conditions. Agric. Water Manag. 50, 53–63.
Wahap, H., Hamid, Y., Tashpulat, T., 2004. Tendency and driving forces of cultivated land use change in Qira oases: the case of Oira oases in south of Tarim basin. Acta Geograph. Sin. 59, 608–614.
Wang, Y., Li, Y., 2010. Transformation of soil salinity in irrigational regions and cropland security: a case study in agricultural oasis of the Sangong River catchment. Arid Land Geogr. 33 (6), 896–903.
Wang, Y.G., Li, Y., 2013. Land exploitation resulting in soil salinization in a desert–oasis ecotone. Catena 100, 50–56.
Wang, Y.G., Li, Y., Xiao, D.N., 2008a. Catchment scale spatial variability of soil salt content in agricultural oasis, Northwest China. Environ. Geol. 56, 439–446.
Wang, Y., Xiao, D., Li, Y., Li, X., 2008b. Soil salinity evolution and its relationship with dynamics of groundwater in the oasis of inland river basins: case study from the Fubei region of Xinjiang Province, China. Environ. Monit. Assess. 140, 291–302.
Wang, Y.Q., Zhang, X.C., Huang, C.Q., 2009. Spatial variability of soil total nitrogen and total phosphorus under different land uses in a small watershed on the Loess Plateau, China. Geoderma 150, 141–149.
Wichelns, D., Qadir, M., 2015. Achieving sustainable irrigation requires effective management of salts, soil salinity, and shallow groundwater. Agric. Water Manag. 157, 31–38.
Xinjiang Institute of Desert and Soil Chinese Academic Sciences, 2000. Xinjiang Soil and Its Utilization. China Science Press, Beijing (in Chinese).
Yan, K., Shao, H.B., Shao, C.Y., Peng, C., Zhao, S.J., Brestic, M., et al., 2013. Physiological adaptive mechanisms of plants grown in saline soil and implications for sustainable saline agriculture in coastal zone. Acta Physiol. Plant. 35, 2867–2878.
Yang, F., An, F., Ma, H., Wang, Z., Zhou, X., Liu, Z., 2016. Variations on soil salinity and sodicity and its driving factors analysis under microtopography in different hydrological conditions. Water 8, 227.
Yeo, A., 1999. Predicting the interaction between the effects of salinity and climate change on crop plants. Hortic. Sci. 78, 159–174.
Yu, S.P., Yang, J.S., Liu, G.M., 2009. Study on prevention and control of secondary soil salinization under intensifying irrigation and straw returning in Huang-Huai-Hai Plain farmland. J. Irrig. Drain. 28, 1–4.
Zhang, Z., Hu, H.C., Tian, F.Q., Hu, H.P., Yao, X.H., Zhong, R.S., 2014a. Soil salt distribution under mulched drip irrigation in an arid area of northwestern China. J. Arid Environ. 104, 23–33.
Zhang, Z., Abuduwaili, J., Yimit, H., 2014b. The occurrence, sources and spatial characteristics of soil salt and assessment of soil salinization risk in Yanqi Basin, Northwest China. PLoS One 9 (9), e106079.
Zhou, D., Lin, Z., Liu, L., Zimmermann, D., 2013. Assessing secondary soil salinization risk based on the PSR sustainability framework. J. Environ. Manag. 128, 642–654.